



Seasonality of the Microbial Community Composition in the North Atlantic

Luis M. Bolaños^{1*}, Chang Jae Choi^{2,3,4}, Alexandra Z. Worden^{2,3}, Nicholas Baetge⁵, Craig A. Carlson⁵ and Stephen Giovannoni^{1*}

¹ Department of Microbiology, Oregon State University, Corvallis, OR, United States, ² Monterey Bay Aquarium Research Institute, Monterey, CA, United States, ³ Ocean EcoSystems Biology Unit, GEOMAR Helmholtz Centre for Ocean Research, Kiel, Germany, ⁴ Marine Science Institute, The University of Texas at Austin, Port Aransas, TX, United States, ⁵ Department of Ecology, Evolution and Marine Biology, Marine Science Institute, University of California, Santa Barbara, Santa Barbara, CA, United States

OPEN ACCESS

Edited by:

Tilmann Harder, University of Bremen, Germany

Reviewed by:

Jarone Pinhassi, Linnaeus University, Sweden Eva Sintes, University of Vienna, Austria

*Correspondence:

Luis M. Bolaños bolanosl@oregonstate.edu Stephen Giovannoni Steve.giovannoni@oregonstate.edu

Specialty section:

This article was submitted to Marine Ecosystem Ecology, a section of the journal Frontiers in Marine Science

Received: 30 October 2020 Accepted: 07 January 2021 Published: 05 February 2021

Citation:

Bolaños LM, Choi CJ, Worden AZ, Baetge N, Carlson CA and Giovannoni S (2021) Seasonality of the Microbial Community Composition in the North Atlantic. Front. Mar. Sci. 8:624164. doi: 10.3389/fmars.2021.624164 Planktonic communities constitute the basis of life in marine environments and have profound impacts in geochemical cycles. In the North Atlantic, seasonality drives annual transitions in the ecology of the water column. Phytoplankton bloom annually in spring as a result of these transitions, creating one of the major biological pulses in productivity on earth. The timing and geographical distribution of the spring bloom as well as the resulting biomass accumulation have largely been studied using the global capacity of satellite imaging. However, fine-scale variability in the taxonomic composition, spatial distribution, seasonal shifts, and ecological interactions with heterotrophic bacterioplankton has remained largely uncharacterized. The North Atlantic Aerosols and Marine Ecosystems Study (NAAMES) conducted four meridional transects to characterize plankton ecosystems in the context of the annual bloom cycle. Using 16S rRNA gene-based community profiles we analyzed the temporal and spatial variation in plankton communities. Seasonality in phytoplankton and bacterioplankton composition was apparent throughout the water column, with changes dependent on the hydrographic origin. From winter to spring in the subtropic and subpolar subregions, phytoplankton shifted from the predominance of cyanobacteria and picoeukaryotic green algae to diverse photosynthetic eukaryotes. By autumn, the subtropics were dominated by cyanobacteria, while a diverse array of eukaryotes dominated the subpolar subregions. Bacterioplankton were also strongly influenced by geographical subregions. SAR11, the most abundant bacteria in the surface ocean, displayed higher richness in the subtropics than the subpolar subregions. SAR11 subclades were differentially distributed between the two subregions. Subclades la.1 and la.3 co-occurred in the subpolar subregion, while la.1 dominated the subtropics. In the subtropical subregion during the winter, the relative abundance of SAR11 subclades "II" and 1c.1 were elevated in the upper mesopelagic. In the winter, SAR202 subclades generally prevalent in the bathypelagic were also dominant members in the upper mesopelagic zones. Co-varying network analysis confirmed the large-scale geographical organization of the plankton communities and provided insights into the

1

vertical distribution of bacterioplankton. This study represents the most comprehensive survey of microbial profiles in the western North Atlantic to date, revealing stark seasonal differences in composition and richness delimited by the biogeographical distribution of the planktonic communities.

Keywords: North Atlantic Aerosols and Marine Ecosystems Study, phytoplankton community composition, bacterioplankton community composition, North Atlantic subregions, seasonal succession, amplicon sequence variants

INTRODUCTION

The phytoplankton spring bloom in the North Atlantic is the climax of an annual cycle driven by the seasonality of physical, chemical and biological features (Sieracki et al., 1993; Behrenfeld and Boss, 2018). This massive pulse in biological productivity is a key mediator of the strength of the biological carbon pump (Martin et al., 2011; Sanders et al., 2014). The phytoplankton spring bloom represents a pathway by which atmospheric CO₂ is biologically converted to organic matter and subsequently exported vertically to depth via sinking particles, vertically migrating zooplankton, and the physical mixing of suspended organic particles and dissolved organic matter (DOM) (Ducklow et al., 2001).

A dynamic ecological system underlies the annual cycle of phytoplankton biomass in the western North Atlantic. Phytoplankton composition has been observed to undergo major seasonal shifts (Choi et al., 2020; Kramer et al., 2020; Yang et al., 2020). Communities dominated by cyanobacteria, prasinophytes and pelagophytes in the early winter give way to a more diverse eukaryotic phytoplankton community in the spring. Major contributors over this period include haptophytes, diatoms, and prasinophytes (Bolaños et al., 2020). The magnitude and composition of springtime diversity captured depends on the successional stage of the phytoplankton bloom that is sampled, which is strongly influenced by both timing and location. Assessing the role of the spring phytoplankton bloom in the biological carbon pump and how it may change in future climate scenarios requires better understanding of the composition, functioning, and interactions of the microbial community.

Bacterioplankton composition in the surface waters of the ocean is influenced by multiple environmental factors and biological interactions (Bunse and Pinhassi, 2017). Seasonality of bacterioplankton has been well documented with interannual time-series in different oceanic regions (Giovannoni and Vergin, 2012; Cram et al., 2015). Transect surveys have provided insights on how bacterioplankton assemblages are biogeographically defined (Milici et al., 2016), and vertical profiles have shown that a high degree of bacterioplankton specialization exists in the water column macro- (Giovannoni et al., 1996; Field et al., 1997; DeLong et al., 2006; Treusch et al., 2009) and micro-environments (Moeseneder et al., 2001; Liu et al., 2018). Bacterioplankton community composition can be influenced by changes in phytoplankton composition, as demonstrated by a bloom study in which cultures of either diatoms or dinoflagellates were inoculated into mesocosms (Camarena-Gómez et al., 2018). Shifts in bacterioplankton

composition are likely, largely determined by variance in the quality and bioavailability of DOM produced by phytoplankton (Aluwihare and Repeta, 1999; Meon and Kirchman, 2001). Variability in DOM composition may result not only from differences in the DOM that distinct phytoplankton release, but also from food-web processes stimulated by phytoplankton community structure. Phytoplankton direct release, grazermediated production, solubilization of sinking and detrital particles, and cell lysis by viral or bacterioplankton infection all affect the magnitude and quality of DOM production (Thornton, 2014; Carlson and Hansell, 2015). Bacterioplankton communities are sensitive and respond to such variability in DOM composition (Massana et al., 2001; Carlson et al., 2002; Liu et al., 2020a). Indeed, microbial DOM remineralization experiments have demonstrated that the amendment of DOM derived from distinct primary producers can differentially affect the responding bacterioplankton community (Nelson et al., 2013; Wear et al., 2015b; Liu et al., 2020b). Coastal surveys observed that bacterioplankton responses to phytoplankton blooms consisted of a succession of different phylogenetic groups driven by the availability of specific classes of algal primary products (Teeling et al., 2012; Wear et al., 2015a). As physicochemical gradients shape phytoplankton communities, these studies collectively demonstrate that shifts in phytoplankton community composition can dictate bacterioplankton species succession on time scales as short as days (Wear et al., 2015a; Needham and Fuhrman, 2016). In this analysis, we hypothesize that seasonal shifts and regional differences in phytoplankton communities through annual cycles shape the composition of heterotrophic bacterioplankton in the North Atlantic.

The North Atlantic Aerosols and Marine Ecosystems Study (NAAMES) was designed to study the plankton ecosystem dynamics over four stages of the annual phytoplankton productivity cycle: early winter ("winter transition": November-December), early spring (early "accumulation phase": March-April), late spring ("climax transition": May-June), and early autumn ("depletion phase": September) (Behrenfeld et al., 2019). Meridional transects sampled water masses originating from the Sargasso Sea, subtropical, temperate and subpolar subregions (Della Penna and Gaube, 2019). In this study, we demonstrate seasonality in microbial composition within the NAAMES region. A near complete view of bacterioplankton and eukaryotic phytoplankton is provided by high-throughput amplicon sequencing of 16S rRNA genes of bacterioplankton and eukaryotic chloroplasts. Samples were collected from eight different depths spanning the euphotic

zone (5–100 m) and upper mesopelagic (150–300 m) at each station. Ecological analyses of Amplicon Sequence Variants (ASVs) maximized the taxonomic resolution of the microbial community variation. Furthermore, ASV co-variability was examined by network analysis to identify large-scale trends in microbial community structure.

MATERIALS AND METHODS

Sampling and DNA Extraction

Microbial biomass was sampled along the meridional transects of the four seasonal NAAMES field campaigns (Figure 1). In early winter (NI; November 2015) and late spring (NII; May 2016), transect sampling covered the subpolar, temperate and subtropical subregions. One station in subtropical waters in the late spring (NII-S4) was sampled daily for 4 days, capturing a local bloom resulting from mixed-layer stratification following a storm-induced deep-mixing event (Graff and Behrenfeld, 2018; Morison et al., 2019; Della Penna and Gaube, 2020). In early autumn (NIII; September 2017), stations covered all four subregions. During this field campaign, one station in the subpolar subregion (NIII-S6) was sampled daily for 4 days. In early spring (NIV; March-April 2018), all stations were located south of 45°N (Figure 1c), spanning the subtropical and Sargasso Sea subregions. Full description of NAAMES campaigns, locations of the stations, hydrographic and environmental data can be found in Behrenfeld et al. (2019). At all stations, 8 nominal depths (5, 25, 50, 75, 100, 150, 200, and 300 m) were sampled at dawn from 10 L Niskin bottles affixed to a standard Conductivity-Temperature-Depth (CTD, Sea-Bird 911+) rosette. At each depth, 4 L of water were collected into a polypropylene carboy (rinsed 3 times with sample water prior to collection). Seawater was then filtered inline using an eightchannel peristaltic pump at a flow-rate of 30 mL/min through a 0.22 µm pore-size Sterivex filter cartridge (polyethersulfone membrane, Millipore). One ml of sucrose lysis buffer (SLB) was added to each cartridge and filters were stored at -80°C until further processing. DNA was extracted from the filters using a phenol:chloroform protocol (Giovannoni et al., 1996). DNA concentration was measured using Quant-iT assays (Invitrogen, Carlsbad, CA) in a Qubit fluorometer. Negative controls consisted of one ml aliquots of the SLB used to preserve the samples for each cruise. DNA extractions, amplicon library preparation, and sequencing of negative controls were performed using the same parameters and protocols used for the samples. Environmental data, as well as data for total chlorophyll a concentration and bacterioplankton abundance, were obtained from the publicly available SeaWiFS Bio-optical Archive and Storage System (SeaBASS)1.

Library Preparation and Amplicon Sequencing

The hypervariable V1-V2 region of the 16S rRNA gene was amplified with the 27F (5'-AGAGTTTGATCNTGGCTCAG-3)

(Lane, 1991) and 338 RPL (5'-GCWGCCWCCCGTAGGWGT-3') (Daims et al., 1999; Vergin et al., 2013) primers attached to Illumina overhang adapters (Illumina Inc.). These primers retrieve V1-V2 16S rRNA gene sequences from bacteria and plastids of multiple phytoplankton lineages in one round of amplification (Rappé et al., 1998). Libraries for each reaction product were constructed by attaching dual indices with the Nextera XT Index Kit (Illumina Inc.) using a second PCR amplification (following manufacturers conditions). Library PCR size was confirmed in a Bioanalyzer DNA 1000 chip (Agilent, Santa Clara, CA, United States). All PCR reactions were purified using AMPure XP beads (Beckman Coulter, Brea, CA, United States). Purified libraries were pooled in equimolar concentrations for each campaign. Each pool was sequenced using the Illumina MiSeq platform (reagent kit v.2; 2 × 250 PE; Illumina Inc.) at the Center for Genome Research and Biocomputing (Oregon State University, Corvallis, Oregon, United States).

Bioinformatics Analysis

Primer sequences from de-multiplexed raw paired-end fastq files were cut using the CutAdapt software (Martin, 2011), removing 20 bases from forward files and 18 from reverse files that matched the 27F and 338 RPL primer lengths, respectively. Trimmed fastq files were quality filtered, dereplicated and merged with dada2 R package, version 1.2 (Callahan et al., 2016) following the pipeline described in Bolaños et al. (2020). Taxonomic assignment was determined aligning the sequences to the silva_nr_v123 database (Quast et al., 2012). ASVs assigned as plastid and cyanobacteria were extracted and placed in curated reference trees (Sudek et al., 2015; Choi et al., 2017) using Phyloassigner version v6.166 (Vergin et al., 2013). Of the negative controls, only the SLB from NAAMES 4 (NIV-SLB_neg) retrieved amplicon sequences. We analyzed the prevalence of potential contamination ASVs with the decontam package (Davis et al., 2018). For phytoplankton community composition, only samples shallower than 100 m that had ≥ 1,600 plastid and cyanobacteria reads were considered. Bacterioplankton sequences of SAR202 clades were further classified using Phyloassigner and custom phylogenetic trees (Vergin et al., 2013; Landry et al., 2017). SAR11 sequences were assigned using a 16S rRNA full-length custom phylogenetic tree. Briefly, we retrieved all SAR11 sequences from SILVA database version SSU r138 which fulfilled the following conditions: taxonomy = "SAR11 clade", sequence length > 1,200 bp, sequence quality > 90. The retrieved set of sequences were aligned using Clustal W (Thompson et al., 1994) and cropped to the last base pair of the 27F primer and position 1,355. Sequences not spanning this region were discarded. Final dataset was composed of 1,181 sequences including those used as outgroup. For the SAR202 tree, we referenced the phylogenetic tree shown in the Figure S1 supplementary data of Landry et al. (2017). We used the setupdb.pl script provided in Phyloassigner to create both phylogenetic databases. SAR11 (Supplementary Figure 1) and SAR202 (Landry et al., 2017) phylogenetic databases along with a metadata table of the SAR11 sequences are available at https://www.github.com/lbolanos32/NAAMES_2020. For

¹https://seabass.gsfc.nasa.gov/naames

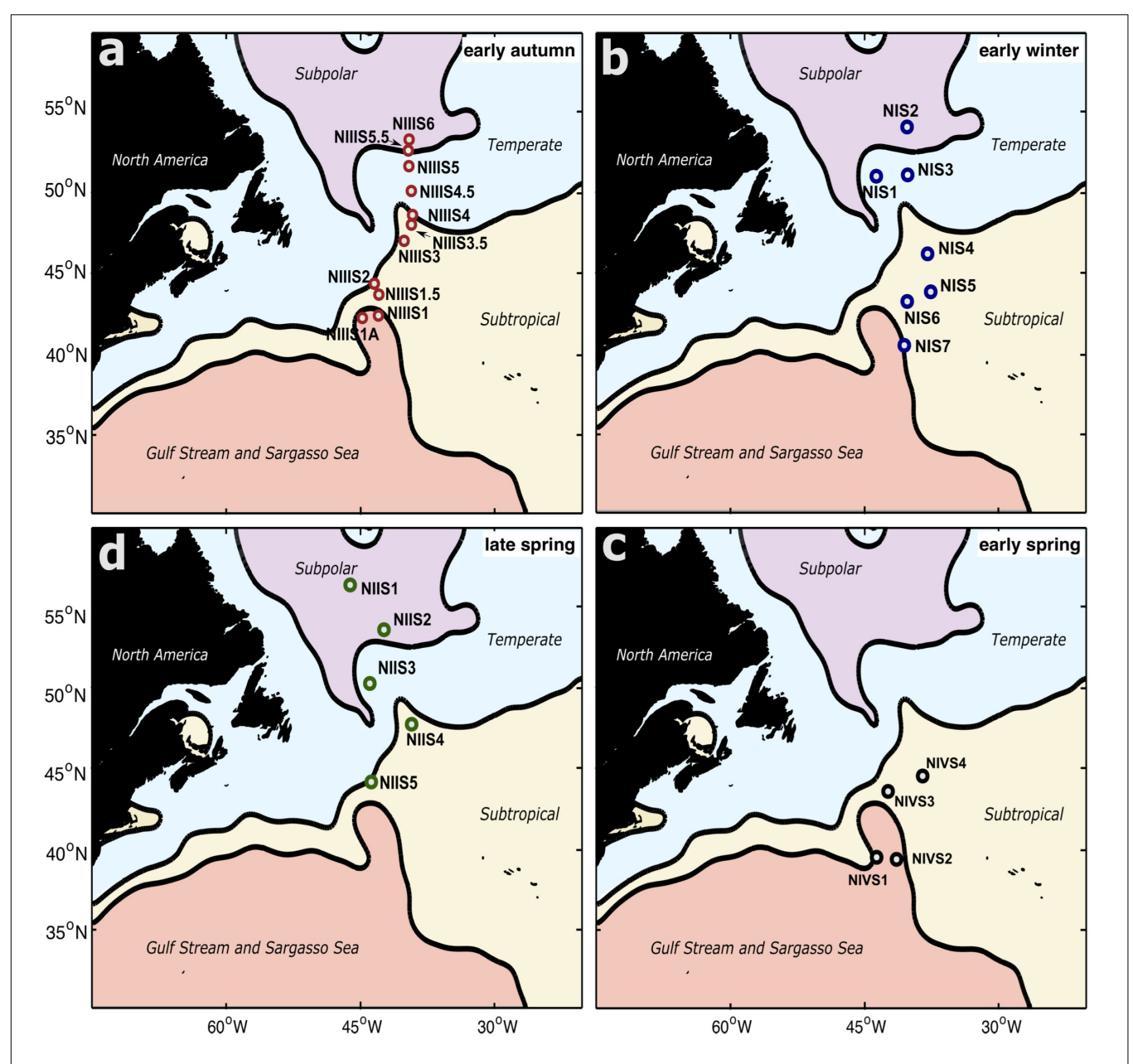


FIGURE 1 | Map of the sampled stations in the western North Atlantic overlapped with the subregions established by Mean Dynamic Topography analysis. Panels in clockwise direction: (a) early autumn (NAAMES field campaign NIII: September 2017) (b) early winter (NAAMES field campaign NII: November 2015) (c) early spring (NAAMES field campaign NIIV: April-March 2018) (d) late spring (NAAMES field campaign NIII: May 2016).

bacterioplankton analysis we included all amplicon datasets composed of \geq 15,000 reads.

Hierarchical clustering (method = "ward.D2") of the phytoplankton fraction was performed with normalized counts using the variance stabilizing transformation in DESEq2 (Love et al., 2014) with fixed zero-tolerant geometric means. Chao1 index and Bray-Curtis dissimilarities were calculated using rarefied datasets (1,600 for phytoplankton and 30,000 for bacterioplankton) with Phyloseq (McMurdie and Holmes, 2013). For SAR11 richness estimation (Chao1), the dataset was rarefied to the minimum in the sample (6,740 sequences). Ordinations

were constructed with the MDS method using the Bray-Curtis dissimilarities. Relative contribution barplots and supporting plots were done in R using ggplot2 (Wickham, 2016) and edited in inkscape² for aesthetics.

Network Analysis, Visualization, and Module Identification

Co-variation network analysis was performed using a reduced dataset to reduce the noise of low abundance ASVs. ASVs

²www.inkscape.org

with less than 6 counts in at least 10% of the samples for the phytoplankton and in 40% of the samples for bacterioplankton were removed. After separately filtering the phytoplankton and bacterioplankton, both datasets were embedded in phyloseq objects and merged. The covarying network was calculated with the SPIEC-EASI function in the SpiecEasi package v.1.0.7 (Kurtz et al., 2015) in R using the Meinshausen-Buhlmann Neighborhood Selection method (50 repetitions). Log2 of the mean of each ASV was calculated to represent the size of the nodes. The network visual representation was achieved with igraph v.1.0.1 (Csárdi and Nepusz, 2006) and ggnet v.0.1.0 (Butts, 2019) packages. Modules were defined using the igraph fast greedy modularity optimization algorithm. The network visualization of each module was done using igraph v.1.0.1 and ggnet v.0.1.0 packages. Supporting heatmap and barplots were generated in R using ggplot2 and edited for aesthetics in inkscape².

RESULTS

Phytoplankton Composition Displays Subregional Seasonality

Profiles of phytoplankton community composition in the euphotic zone (upper 100 m) were analyzed along the meridional transects of the four campaigns, each capturing distinct stages of the phytoplankton productivity annual cycle (Figure 1). Previous observations from the early winter (Figure 1b) and late spring (Figure 1d) campaigns revealed two distinctive phytoplankton communities (Bolaños et al., 2020). One group was characterized as subpolar for samples collected in the subpolar and temperate subregions, the other as subtropical for samples collected in the subtropical and Gulf stream-Sargasso Sea subregions. The present study adds the analysis of phytoplankton composition datasets from the early autumn (Figure 1a) and early spring (Figure 1c). Clustering based on the ASV profiles revealed that early spring and early autumn phytoplankton communities generally differentiated into the two groups matching the previously described subpolar and subtropical community types (Supplementary Figure 2). However, the early autumn subtropical samples did not cluster with the other seasons from the subtropical subregion, instead clustering more closely to the subpolar grouping.

Multidimensional scaling (MDS) based on Bray-Curtis dissimilarities (beta diversity) supported the observed clustering pattern in phytoplankton surface communities, resolving further details of each campaign (Figure 2A and Supplementary Figure 3). In early autumn and early winter, sample clustering followed a north to south organization, represented by the second axis (Figure 2A). Early autumn samples showed a gradient of latitudinal distribution with some overlaps between the subtropical and subpolar communities. During early winter, a larger separation clearly distinguished the subpolar and subtropical communities. The latitudinal ordination observed in the early autumn and early winter communities was shifted in the early spring. Subtropical early spring samples organized by

longitude, with stations 1 and 3 (43°W, 42°W, respectively) being more similar to each other than either with 2 and 4 (41°W, 38°W, respectively).

Total chlorophyll a concentration was used as a proxy for phytoplankton biomass and remained below 2 mg/m³ throughout all sampled stations (Figure 3), with one exception. In the subpolar late spring, surface chlorophyll a concentrations were maximal, increasing southward from 56° N to 50° N. This pattern reflects the general timing phenomenon where the peak of the bloom shifts to later dates with increasing latitude. Phytoplankton-derived 16S rRNA gene copies retrieved from the total dataset did not follow the same pattern as chlorophyll a concentrations. Low chlorophyll samples were not necessarily associated with a low number of phytoplankton gene copies, as shown by the early autumn subtropics (Figure 3). Of the total sequences recovered, the percentage represented by phytoplankton ranged from \sim 5% in the subpolar autumn and winter samples to a maximum of 60% in the subtropical late spring.

Patterns in phytoplankton ASV richness through the water column differed at each station, likely due to the influences of subregional and seasonal conditions (Figure 3). During the subpolar late spring bloom, ASV richness increased in parallel to chlorophyll a concentration. No other season showed a similar effect, indicating that spring bloom conditions allowed a diverse set of phytoplankton to succeed. The lowest richness was observed in samples from both the subpolar early winter and the surface (5-25 m) of the early autumn subtropics. The low ASV richness in these environments at these times reflects different types of limiting conditions to phytoplankton. In the subpolar early winter, low temperature, deep mixing, and low light may restrict the range of phytoplankton species that can thrive. Comparatively, in the thermally stratified water column characteristic of the early autumn subtropics, nutrient depletion may be a more influential factor that skews community composition toward groups better adapted to oligotrophic conditions.

Subpolar phytoplankton communities shifted sharply through seasons. In early autumn, a diverse set of eukaryotic phytoplankton, including cryptophytes, prymnesiophytes, pelagophytes, and bacillariophytes dominated the communities. The remaining sequences were represented by cyanobacteria, specifically *Synechococcus* ecotypes I and IV. Early winter was dominated by *Synechococcus* ecotypes I and IV and prasinophytes. During the late spring bloom, cyanobacteria relative abundances decreased, while eukaryotic phytoplankton dominated and were particularly represented by haptophytes, rappemonads, prasinophytes, and bacillariophytes.

Subtropical phytoplankton communities displayed seasonal patterns. Cyanobacteria dominated in the early autumn; *Prochlorococcus* contributions made up to 95% of the phytoplankton reads at the two most southern stations of the subregion. *Prochlorococcus* dominance decreased northward, while the relative abundance of *Synechococcus* clades I and IV increased. In early autumn, eukaryotic sequences were most pronounced at depths greater than 25 m and were primarily composed of prasinophytes. In early winter, prasinophytes

Bolaños et al. North Atlantic Plankton Composition

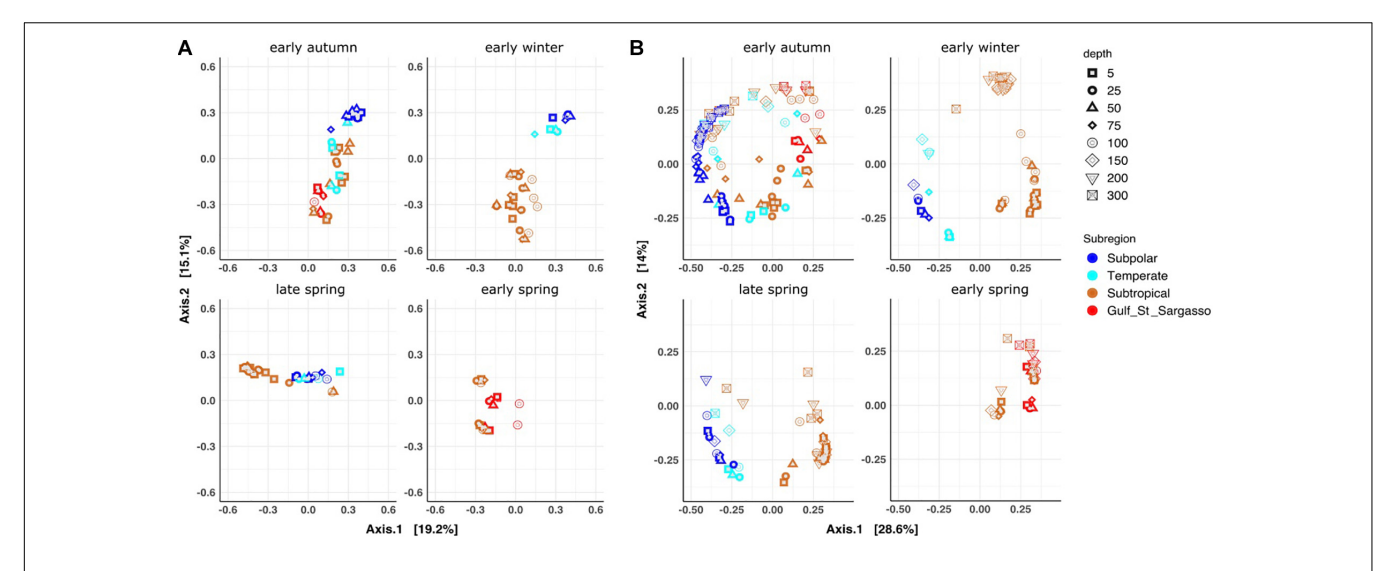


FIGURE 2 | Multidimensional scaling (MDS) ordination based on Bray-Curtis dissimilarities (A) Phytoplankton fraction of the datasets (0–100 m) (B) Bacterioplankton fraction of the datasets (0–300 m). Ordinations were divided in four panels representing each of the sampled seasons (clockwise: early autumn, early winter, early spring, late spring). Datasets in both panels are colored based on the MDT subregion.

increased relative to early autumn throughout the euphotic zone and, with cyanobacteria, dominated the communities. The cyanobacterial fraction at this time was dominated by Prochlorococcus HL l and Synechococcus IV. In the early spring, Synechococcus (clades II and IV) and prasinophytes dominated, but bacillariophytes and prymnesiophytes increased to comprise up to 25% of the ASVs. In the late spring, the two stations that were sampled in the subtropical subregion had distinct communities from each other. NII-S4 was a unique station in that it was homogeneously mixed to > 250 m upon the first day of occupation and stratified to < 50 m over the next 4 days of occupation. As the water column stratified at NII-S4, the relative abundance of phytoplankton sequences became dominated by prasinophytes and diatoms, both of which increased in cell number. In contrast, the subtropical station NII-S5, which was thermally stable and stratified, showed an increase in the relative contribution of Synechococcus, which made up to 35% of the sequences.

Overall, the annual phytoplankton seasonality showed two distinct patterns of community succession specific to each subregion. In the subpolar subregion, eukaryotes displayed broad taxonomic shifts accompanied with a variable seasondependent contribution of cyanobacteria, specifically constrained to the co-occurrence of Synechococcus clades I and IV. Cyanobacteria contribution in this subregion displayed a maximum in winter. Comparatively, eukaryotic phytoplankton composition was broad and relatively stable in the subtropics throughout the year, mostly being of prasinophytes (Bathycoccus, Ostreococcus, and Micromonas) and bacillariophytes. In this subregion, the contribution of cyanobacteria shifted sharply between seasons, reaching a maximum in early autumn. Common to both subregions, eukaryotes displaced cyanobacteria to marginal contributions and dominated phytoplankton bloom communities during the late spring.

Bacterioplankton Community Composition

Bacterioplankton profiles spanning the surface 300 m were analyzed by subregions and seasons to assess whether or not similar spatiotemporal patterns exist between phytoplankton and bacterioplankton community composition (Figure 2). MDS ordination, based on Bray-Curtis dissimilarities, showed that bacterioplankton communities geographically clustered in a similar pattern as the phytoplankton communities. Subtropical and Gulf stream - Sargasso Sea communities clustered together (i.e., subtropical community), while subpolar and temperate communities clustered together (i.e., subpolar community) (Figure 2B and Supplementary Figure 4). As expected, bacterioplankton communities were structured by depth at almost all seasons and stations, with samples from the euphotic zone (<100 m) generally ordinating distantly from those in the upper mesopelagic (150-300 m; Axis 2). However, the magnitude and depth of the transition differed by station and with season. In early autumn, bacterioplankton communities clustered by subregion and depth, but an overlap in community structure between subregions was observed, similar to the phytoplankton ordination. In the early winter, communities clustered clearly and distantly by subregion and by location within the water column. Samples from the wintertime subtropical mesopelagic clustered tightly to each other and distally from others, reflecting a similarly unique composition in their community structure, while the wintertime subpolar samples showed a more subtle differentiation between the euphotic and upper mesopelagic. In early and late spring, bacterioplankton communities transitioned gradually from the euphotic zone to the mesopelagic. An exception to this was at NII-S4, where a mostly homogeneous community was observed over 200 m due to a recent storm-induced

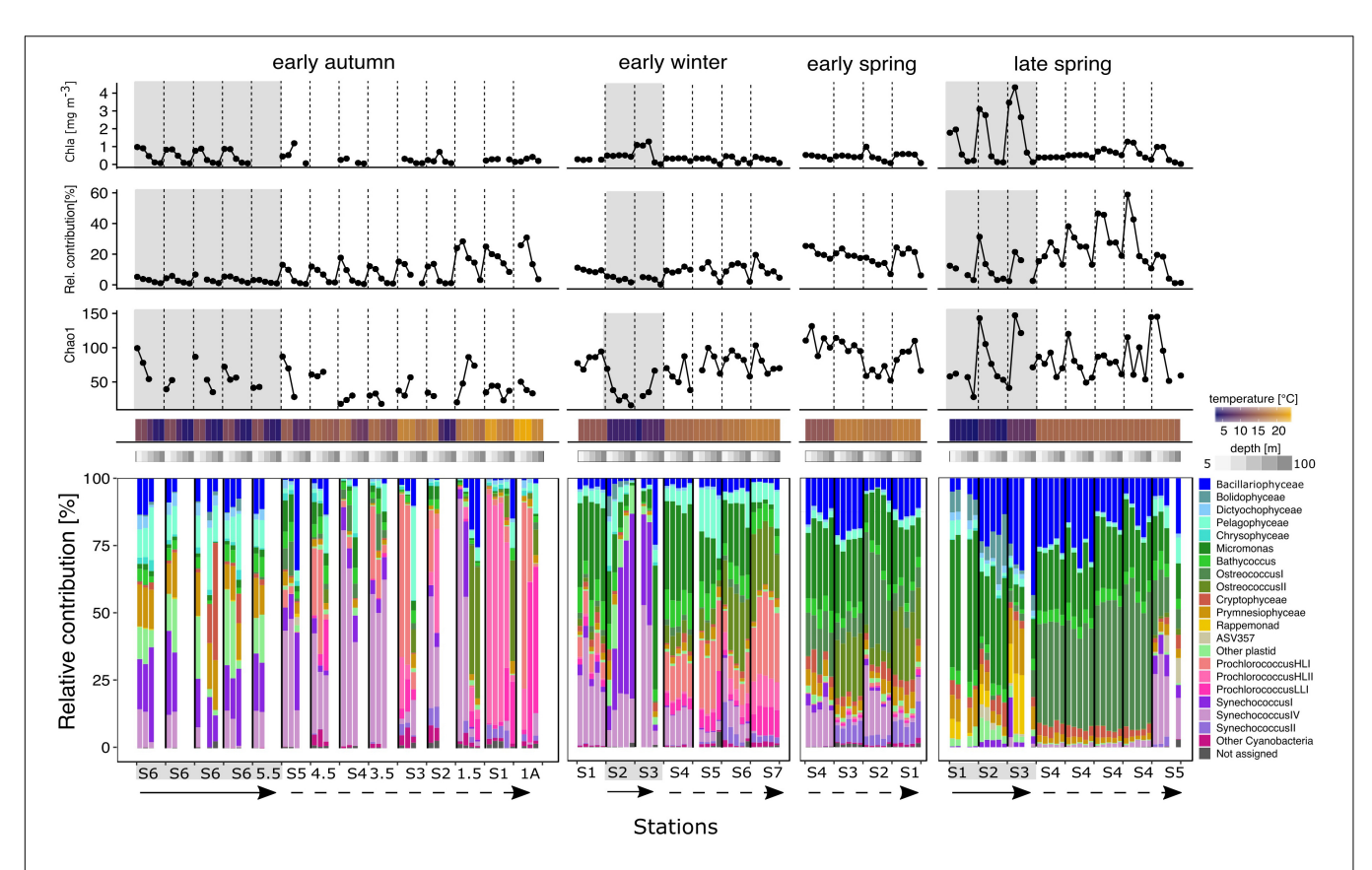


FIGURE 3 | Environmental metadata and stacked bar plots of the taxonomic relative contributions to the phytoplankton fraction for each station within each seasonal campaign. Top three panels: Chlorophyll a concentration (uppermost), phytoplankton relative contribution to the total sequences (middle) and Chao 1 richness (bottom). Data points in the three line graphs are aligned to the phytoplankton community composition representation below. Bottom panel: stacked barplot representing the relative contributions of the different taxonomic groups to the phytoplankton fraction. Bars are organized by station from left to right in a north to south direction indicated by the straight arrow (subpolar) and the dashed arrow (subpolar), except early winter where S2 was the most northern station. Only depths 5–100 m were analyzed and plotted for the phytoplankton fractions. Within each station, depths are organized in a descending order from 5 to 100 m in a left to right direction. Blank columns represent samples that did not overcome the minimal sequences threshold or where sample failed to generate amplicon sequences. Temperature and depth heatmap cells and data points in the three line charts correspond to the sample represented by the aligned barplot below these. Gray background shading indicates that the profile is biologically categorized as subpolar (physically located in the subpolar and temperate), while no shades represents subtropical (physically located in the subtropical and Sargasso Sea).

deep mixing event (mixed layer depth of > 250 m), mentioned previously.

Bacterioplankton abundance (cells/L) near the surface (5 and 25 m) was lower in the early winter and early spring compared to late spring and early autumn (Figure 4). Bacterioplankton ASV richness was lower in subpolar subregions than subtropical subregions (Figure 4). Seasonality and latitude influenced richness patterns throughout the water column for both subregions. In early autumn, all stations displayed similar richness profiles to each other, increasing gradually with depth. Early winter displayed a different pattern where subtropical communities showed the highest richness of all samples, especially in the upper mesopelagic. In contrast, the early winter subpolar stations had the lowest richness. The two most northern subtropical stations in the early spring showed constant richness throughout the water column, while richness increased with depth at the southern stations. In the late spring, richness increased southward and followed the phytoplankton bloom progression.

The SAR11 clade was the dominant fraction of the bacterioplankton community across space and time (Figures 4-6). However, SAR11 ASV richness was lower in the subpolar subregion compared to the subtropics, following the total bacterioplankton abundance (Figures 4, 5) and richness (Figure 6). SAR11 subclades, thought to be ecotypes with specialized adaptations, displayed different spatiotemporal distributions in the euphotic zone and the upper mesopelagic (Figure 6). Subclades Ia.1 and Ia.3 dominated the community in the euphotic zone through most seasons, with clear subregional differences in relative abundances. SAR11 subclade Ia.1 was co-occurrent with Ia.3 in the subpolar subregion regardless of the season, while the relative contribution of subclade Ia.3 dominated throughout the subtropics. In the subpolar subregion, subclades IIa.B and IV made the rest of the SAR11 fraction. These subclades showed a decreasing contribution from more than 30% of the SAR11 clade in the early autumn to less than 10% in the late spring, when Ia.1 and I.a3 dominated the subpolar euphotic zone. Throughout the year in the subtropics, multiple subclades

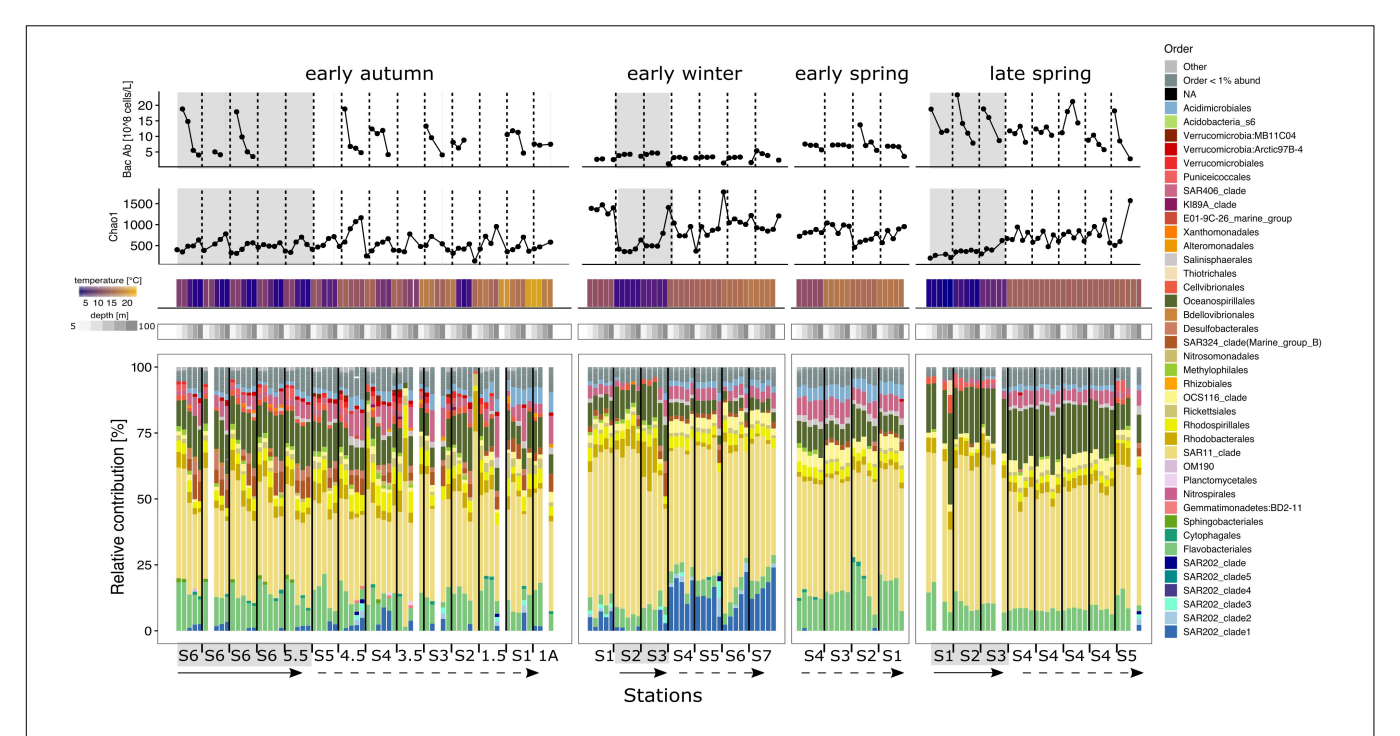


FIGURE 4 | Environmental metadata and stacked bar plots of the taxonomic relative contributions to the bacterioplankton fraction for each station within each seasonal campaign in the euphotic zone. Top two panels: bacterioplankton abundance and Chao 1 richness. Temperature and depth heatmap cells and data points in the three line charts are aligned to the bacteria community composition representation below. Base barplots depict the relative contributions of the different taxonomic groups within the bacterioplankton fraction. Bars are organized by station from left to right in a north to south direction indicated by the straight arrow (subpolar) and the dashed arrow (subpolar), except early winter where S2 was the most northern station. Depths 5–100 m were analyzed and plotted for the bacterioplankton fractions. Within each station, depths are organized in a descending order from 5 to 100 m following a left to right direction. Blank columns represent samples that did not overcame the minimal sequences threshold or which sample was unsuccessful to generate amplicon sequences. Gray background shading indicates that the profile is biologically categorized as subpolar, while no shades represents subtropical.

including Ia.4, Ib.1, Ib.2, Id, IIa.A, and IIa.B accompanied the dominant Ia.1. Of these subclades, Ib.1 and Ib.2 were the most sensitive to seasonal changes, being abundant in early winter and spring and then decreasing in the autumn to a negligible fraction of the SAR11 clade.

Subclades Ia.1 and Ia.3 dominated the upper mesopelagic and displayed similar ratios between subregions. In early autumn, the SAR11 composition across the subpolar and subtropical regions were homogenous. Notably, sequences belonging to the subclade II made more than 30% of the SAR11 clade in the upper mesopelagic. By the early winter in the subtropics, subclade II increased up to 40%. Subclade 1c.1 was also observed to increase to more than 10% at this time within the upper mesopelagic. In the early and late spring, SAR11 composition was similar between the upper mesopelagic and the euphotic zone. In station NIV-S3 of early spring, the distribution of SAR11 subclade relative abundance was uniform from 5 to 300, while at stations 1 and 2, clade II relative abundance gradually increased with depth. At NII-S4 in the late spring, an initially homogenous SAR11 composition through the water column changed, with the relative contribution of subclades II increasing to the end of the occupation as the water column stratified.

Over the annual cycle in both subregions, bacterioplankton taxa within Flavobacteriales, Oceanospirilalles, SAR406, Acidomicrobiales, and Rhodospirilales, were the next most abundant ASVs after SAR11 in their relative contributions to total bacterioplankton. However, SAR202 became an abundant contributor at subtropical stations in the winter, making up to 53% of the total sequences (300 m, NI-S4; Figure 5). SAR202 sharply increased in depths greater than 100 m, but with shifting subclade composition (Figures 4, 5). For example, SAR202 clade 1 dominated in the euphotic zone, while SAR202 clades 2 and 3 became more prominent in the upper mesopelagic (Figures 4, 5). Additionally, the absence of OCS116 and the reduction of Oceanospirillales in the upper mesopelagic contributed to the sharp shift in vertical community composition in the subtropics during the early winter.

At the most southern stations in early spring, NIV-S1 and NIV-S2, Flavobacteriales made up to 25% of the community in the surface 50 m, but dropped drastically at depths deeper than the euphotic zone. At stations NIV-S3 and NIV-S4, Flavobacteriales were distributed homogenously throughout the water column. During the late spring, Oceanospirillales composed between 10 and 35% of the community at all stations and were the major responders to the increase in phytoplankton biomass in the euphotic zone, but were also prevalent in the upper mesopelagic. In the early autumn, large gradients in community structure across depth were observed. For example, at subpolar NIII-S6, Desulfobacterales and SAR324 increased from being

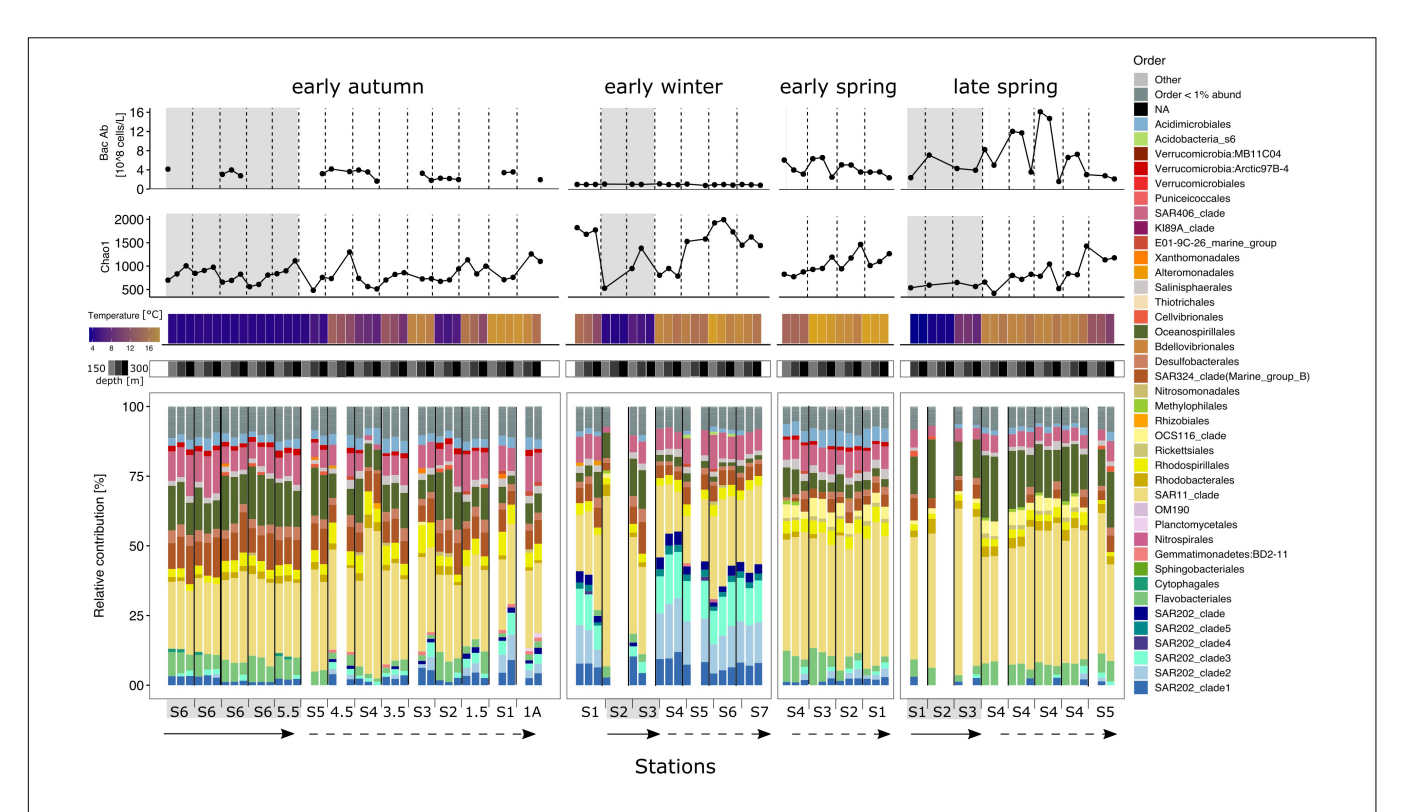


FIGURE 5 | Environmental metadata and stacked bar plots of the taxonomic relative contributions to the bacterioplankton fraction for each station within each seasonal campaign in the upper mesopelagic. Top two panels: bacterioplankton abundance and Chao 1 richness. Temperature and depth heatmap cells and data points in the three line charts are aligned to the bacteria community composition representation below. Base bar plots depict the relative contributions of the different taxonomic groups within the bacterioplankton fraction. Bars are organized by station from left to right in a north to south direction indicated by the straight arrow (subpolar) and the dashed arrow (subpolar), except early winter where S2 was the most northern station. Within each station, depths are organized in a descending order from 150 to 300 m following a left to right direction. Blank columns represent samples that did not overcame the minimal sequences threshold or which sample was unsuccessful to generate amplicon sequences. Gray background shading indicates that the profile is biologically categorized as subpolar, while no shades represents subtropical.

nearly absent in the surface 25~m to together contributing up to 17% of the sequences at 300~m. Notably, from the early spring to the early autumn, SAR202 were marginalized or even absent in the euphotic zone and at 150~and~200~m, but made up between 5 and 9% of the community at 300~m.

Co-variation Network Analysis and Modularity of ASVs

To identify patterns of co-variation among ASVs that might indicate interactions among planktonic taxa or among sets of taxa with adaptations to very similar environments, we constructed a network using the most abundant 292 bacterioplankton (representing 71.2% of the total bacterioplankton reads) and 128 phytoplankton (representing 92.1% of the total phytoplankton reads) ASVs from samples of the upper 100 m of the water column (**Figure 7** and **Supplementary Figure 5**). Overall, the network had a clustering coefficient of 0.1414 indicating it is a sparse network and a graph average degree of 13.295 (total edges/total nodes).

The co-varying network was compartmentalized into 14 modules (Figures 7, 8 and Supplementary Figure S5). Sixty five percent of the phytoplankton ASVs could be found in

only three modules (4, 2, and 9). These modules dominated by phytoplankton ASVs were strongly associated with subregions. Phytoplankton covarying module 4 was mainly constrained to the subpolar subregion and linked with bacterioplankton ASVs related to Oceanospirillales, SAR11 subclade II, and Verrucomicrobia (Figure 8, Supplementary Figure 6, and **Supplementary Table 1**). Phytoplankton covarying module 2 was associated to the subtropical subregion and linked with bacterioplankton ASVs related to Flavobacteriales, SAR406, and SAR11 subclade II (Figure 8, Supplementary Figure 6, and **Supplementary Table 1**). Phytoplankton covarying Module 9 was associated with the most southern stations under the influence of the Gulf Stream and the Sargasso Sea. In this module we found bacteria ASVs belonging to SAR202 clade 1 and SAR86 (Figure 8, Supplementary Figure 6, and Supplementary Table 1). This distinction between subtropical and Sargasso Sea phytoplankton dominated modules indicates a southern ecological boundary not captured by the ordination (Figure 2B) or clustering (Supplementary Figure 2). The more highly resolved sampling of the southern latitudes in early spring and early autumn compared to our previous analysis of the early winter and late spring (Bolaños et al., 2020) helped to define the boundary in the network analysis.

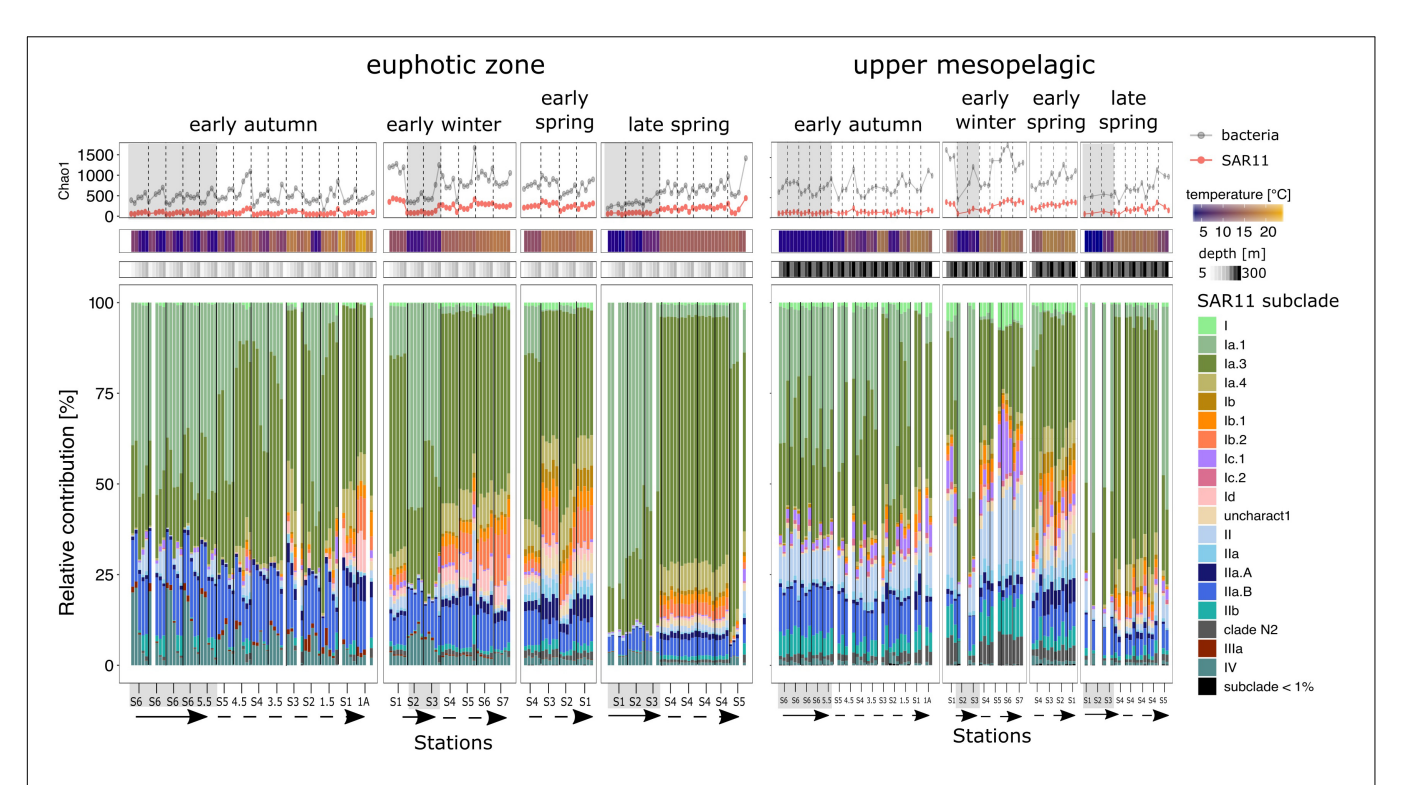


FIGURE 6 | SAR11 richness (Chao1) and stacked bar plots of the subclades relative contributions for each station within each seasonal campaign. Top panel represent the richness (Chao 1 index) of the bacterioplankton fraction (gray line) and the specific to SAR11 ASVs (red line). Base barplots depict the relative contributions of the SAR11 subclades in the euphotic zone (left side) and the upper mesopelagic (right side). Bars are organized by station from left to right in a north to south direction indicated by the straight arrow (subpolar) and the dashed arrow (subpolar), except early winter where S2 was the most northern station. Within each station, depths are organized in a descending order. Blank columns represent samples that did not overcame the minimal sequences threshold or which sample was unsuccessful to generate amplicon sequences. Gray background shading indicates that the profile is biologically categorized as subpolar, while no shades represents subtropical.

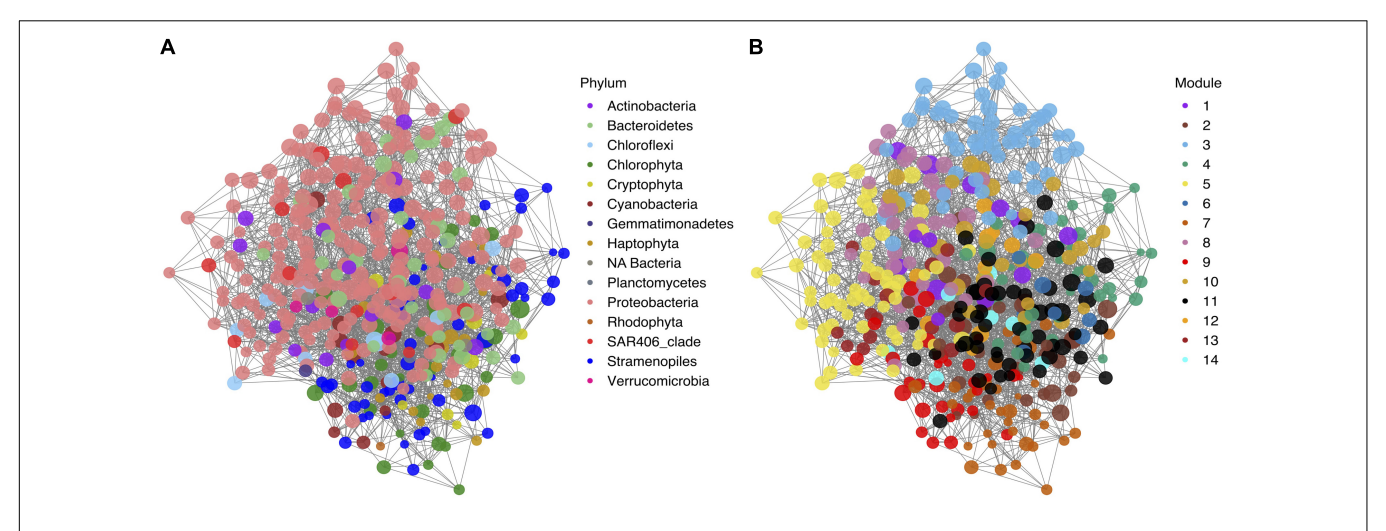


FIGURE 7 | Covariation network of the 128 phytoplankton and 292 bacterioplankton most abundant ASVs and modularity analysis. (A) Visual representation of the non-directed ASVs covariation network. Nodes are color-coded by phylum. (B) Visual representation of the non-directed ASVs covariation network with the nodes color-coded by module. Size of the nodes in both panels depicts the log2 of the represented ASV average.

Modules dominated by bacterioplankton ASVs also showed subregional and seasonal differences in addition to differences according to depth (**Figures 7, 8**). Modules 3 and 10 were found in the subpolar subregion and some subtropical stations

in early autumn. These were mainly composed of Proteobacteria and Bacteroidetes. Subtropical modules 5, 8, and 11 were present in all four seasons. Modules 5 and 8 followed similar distributions, except in early autumn. Module 11 was detected

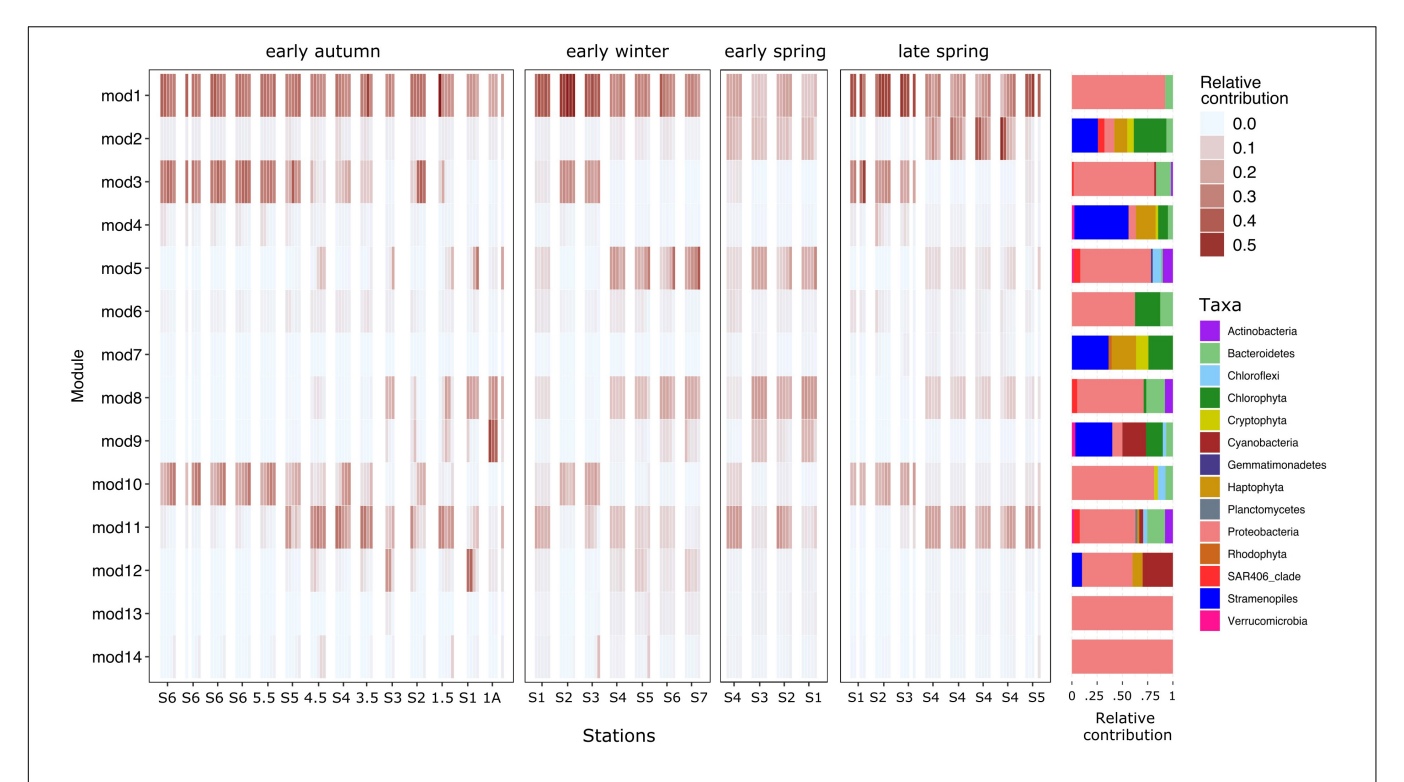


FIGURE 8 | Heatmap depicting the relative contributions in the euphotic zone of each network's module to the total dataset. Modules are organized in sequential numbers from top to bottom in the *x*-axis. Samples are displayed in the *y*-axis; organized following the same order as in **Figures 3–6**. Only ASVs from the upper 100 m samples were analyzed. The percentage represented by the heatmap is restricted to the total reads of ASVs used in the network analysis. Aligned barplots on the right side of the heatmap represent the taxonomic relative contribution of the ASVs to the module.

in subpolar samples and one of the few that overlapped between geographical subregions. Two ubiquitous modules were found: module 1, composed mainly of abundant SAR11 ASVs, and module 6, which contained *Micrococcus*, *Bathycoccus*, and Alphaproteobacteria AEGAN-169 ASVs (Supplementary Figure 6 and Supplementary Table 1).

While the observed network modularity indicates a strong influence of geographical subregions on the phytoplankton community composition, other factors likely influence the high degree of variability between bacterioplankton modules. Phytoplankton underwent major changes over the annual cycle in the subpolar subregion, but these changes could be tracked to a single covarying set of ASVs that were grouped in module 4. Comparatively, the dominant bacterioplankton modules in the subpolar subregion could also be found in the subtropical stations. Bacterioplankton assemblages are not only associated to season or subregion but also with depth (Figure 8).

DISCUSSION

The temperate and subpolar latitudes of the western North Atlantic are dynamic regions that have been under-sampled compared to the eastern region of the basin (Behrenfeld et al., 2019). There is a paucity of microbial community structure data for the western North Atlantic outside of those provided by the large-scale survey projects such as Bermuda Atlantic Time-series

Study (BATS), Tara Oceans (Karsenti et al., 2011; Sunagawa et al., 2020) and Malaspina (Duarte, 2015). The NAAMES field campaign provided the most comprehensive temporal and spatial view of the microbial communities for this region between 39 and 56° N. The sequencing strategy we selected targeted the 16S rRNA V1-V2 hypervariable region and provided information on the relative abundance of heterotrophic bacterioplankton, cyanobacteria and eukaryotic phytoplankton (by means of the plastid 16S rRNA gene) in a single experiment.

Our previous analysis revealed a strong correlation between phytoplankton communities and the hydrographic origin of the water masses where the samples were collected (Bolaños et al., 2020). Although seasonality generates a sharp shift in phytoplankton composition, communities are constrained by the environmental conditions specific to the subregions including the degree of stratification, availability of macronutrients and temperature regime. ASV co-variation network analysis confirmed the strong boundaries that define the communities in this region. Cyanobacteria, prasinophytes and stramenopiles were the phytoplankton groups that shifted the most between seasons. Research based on pigment data extended this observation to Dinoflagellates, which were not efficiently detected by the PCR primers used previously (Kramer et al., 2020). Prasinophytes (green algae picoeukaryotes) had high relative abundance during winter and spring (early and late) but declined in autumn. Photosynthetic picoeukaryote communities have been shown to be sensitive to temperature, light intensity and

nutrient concentrations (Kirkham et al., 2011). Furthermore, increasing numbers of cyanobacteria and their expansion to higher latitudes are predicted as a consequence of global warming (Morán et al., 2010; Flombaum et al., 2013). The contributions of cyanobacteria reported in this study suggests that they may be more competitive than prasinophytes in the oligotrophic and highly stratified subtropical conditions that characterized the most southern autumn NAAMES stations (\sim 42–47° N). One biological characteristic that might favor cyanobacteria is the high surface area to volume ratio of these cells that can make them more competitive at low nutrient concentrations.

Our results add support to the notion that the seasonal succession in ocean bacteria is constrained by the biogeographical distribution of the communities (Bunse and Pinhassi, 2017), but also shows that the succession manifests differently between the euphotic and the upper mesopelagic zones within our study region. The euphotic and upper mesopelagic zones were dominated by SAR11 but the dynamics of SAR11 subclades differed between subpolar and subtropical subregions. The subpolar SAR11 composition was dominated by the co-occurrence of subclades Ia.1 and Ia.3 in all seasons, while only Ia.3 was predominant in the subtropics. It is well documented that subclade Ia.1 is associated with cold environments and Ia.3 to temperate and tropical (Brown et al., 2012; Eren et al., 2013). However, the co-occurrence in the subpolar subregion suggests that subclade Ia.3, or specific phylotyopes within it (Delmont et al., 2019), are adapted to a broader range of temperatures. In the subtropics, SAR11 subclades followed a similar spatiotemporal dynamic as previously reported at BATS site (Carlson et al., 2009; Vergin et al., 2013; Giovannoni, 2017). For example, subclade Ib peaked in the euphotic zone during the period of water column instability from early winter to spring, while subclade II dominated the upper mesopelagic zone following deep convective overturn in the late winter and early spring. Comparatively, SAR11 composition in the subpolar subregion was less dynamic and diverse: subclades Ia.1 and Ia.3 dominated, with subclades IIa.B and IV comprising the remainder of the SAR11 fraction and varying only slightly in relative contributions throughout the seasons.

During the subtropical autumn and winter, upper mesopelagic bacterioplankton differentiated sharply from the euphotic communities, while in the spring (early and late) community composition transitioned more gradually through depth. The largest difference between euphotic and upper mesopelagic communities was in the early winter subtropics. At these stations, SAR202 subclades 2 and 3, which are commonly found in the bathypelagic (Saw et al., 2020), dominated the upper mesopelagic zone. SAR202 genomes encode for paralogs hypothesized to oxidize remnant recalcitrant DOM (Landry et al., 2017; Saw et al., 2020). In the subtropical water masses, where diatoms are displaced by cyanobacteria during highly stratified period, net DOC accumulation is observed (Hansell et al., 2009; Carlson et al., 2010; Romera-Castillo et al., 2016). In the subtropics a greater percentage of net community production is partitioned as accumulating DOC, which can lead to a greater export

potential from the surface into the mesopelagic at latitudes that also experience deep winter convection (Baetge et al., 2020). The differences in DOC accumulation between regions with distinct phytoplankton communities may lead to differences in the quality of organic matter exported to the mesopelagic, contributing to the observed response of SAR202 during or shortly following deep winter convection in the subtropical realm (Treusch et al., 2009).

In autumn, SAR324 and Desulfobacterales increased in the upper mesopelagic. SAR324 are well-known deep ocean chemolithotrophs that have C1 metabolism and a particle-associated lifestyle (Swan et al., 2011), while Desulfobacterales are sulfate-reducing strict anaerobes. Both taxa are well-known inhabitants of the dark ocean, but seasonality has not been documented in these bacteria (Treusch et al., 2009; Nelson et al., 2014; Yilmaz et al., 2016).

In spring, bacterioplankton communities transitioned with depth without the sharp shifts observed in other seasons. These results may suggest that primary production from the euphotic zone creates a gradient of DOM flux. In spring, when primary production was greatest, Flavobacteriales and Oceanospirillales had a high relative contribution in the euphotic zone. The increase in abundance of these taxa concomitant to phytoplankton bloom progression has been reported in other systems, including the northern Antarctic peninsula (Signori et al., 2018) and Antarctic islands in the Southern Indian Ocean (Landa et al., 2016). This suggests that these bacteria might respond to the DOM produced as a result of numerous food web processes that occur during the periods of high primary production. During this season in the subpolar subregion (highest chlorophyll concentrations), bacterioplankton richness represented by the Chao1 index reached the lowest values, while bacterioplankton abundance, phytoplankton biomass, and phytoplankton richness were at their highest values. This suggests that during the peak of primary productivity, specific copiotrophic Rhodobacterales and Flavobacteriales may be responding to the flux of fresh labile DOM, outcompeting other community members as observed during phytoplankton blooms (Buchan et al., 2014; Luria et al., 2017).

Biotic interactions are increasingly recognized as a major influence on planktonic community composition (Lima-Mendez et al., 2015). We analyzed the organization of the communities in co-varying modules using a network analysis. The network delineated 14 covarying modules among the most abundant phytoplankton and bacteria ASVs. These modules reflected subregional and seasonal variation and were congruent with the results of ordination and community clustering. However, the modules were insufficient to resolve potential phytoplankton-bacteria interactions at a local spatial and temporal scales. The tightly varying phytoplankton communities influenced by subregion contrasted to the atomized co-varying bacterioplankton modules, which showed an additional set of patterns, mostly influenced by depth. This evidence may suggest that bacterioplankton are more sensitive to local gradients or disturbances, or that the diversity of heterotrophs is arranged in additional dimensions by factors such as DOM quality and of flux from food web sources.

Our results provide evidence of the profound effect of water mass origin and inherent physical/chemical features on the seasonal dynamics of plankton community composition. In previous work phytoplankton communities have been ordered in reference to large-scale subregions of the North Atlantic (Bolaños et al., 2020). Although bacterioplankton composition is restricted by the same ecological borders as phytoplankton, seasonal fluctuations in the water column and primary production determine how the community transitions are shaped through depth. This effect creates a dynamic system, sensitive to phytoplankton community changes but not strictly correlated in the same temporal scale.

DATA AVAILABILITY STATEMENT

Amplicon sequence datasets presented in this study have been deposited in NCBI SRA database under the BioProject identifier PRJNA627189.

AUTHOR CONTRIBUTIONS

LB and SG conceived the study and experimental design, collected the samples, and generated the sequence data. LB, CC, and NB analyzed the data. All authors contributed to the writing, revision, and editing of the final manuscript.

FUNDING

This research was supported by the NASA grant no. NNX15AE70G to SG, award NSF OCE-157943 to CC and NSF Dimensions Collaborative Research grant: Unraveling thiamin cycling complexity and impacts on microbial networks to SG (DEB-1639033), and AW (DEB-1638928). This work was funded by Simons Foundation International as part of the BIOS-SCOPE initiative (SG).

ACKNOWLEDGMENTS

We thank Mark Dasenko and the members of the Oregon State University Center for Genome Research and Biocomputing (CGRB) for library preparation, sequencing and maintenance of the computational infrastructure. We thank Captains A. Lund and D. Bergeron and *R/V* Atlantis crew. We thank Michael Behrenfeld for leading NAAMES. We thank NAAMES participants for core data and their feedback to this study.

REFERENCES

Aluwihare, L. I., and Repeta, D. J. (1999). A comparison of the chemical characteristics of oceanic DOM and extracellular DOM produced by marine algae. Mar. Ecol. Prog. Ser. 186, 105–117. doi: 10.3354/meps186105

Baetge, N., Graff, J. R., Behrenfeld, M. J., and Carlson, C. A. (2020). Net community production, dissolved organic carbon accumulation, and vertical export in

SUPPLEMENTARY MATERIAL

The Supplementary Material for this article can be found online at: https://www.frontiersin.org/articles/10.3389/fmars. 2021.624164/full#supplementary-material

Supplementary Figure 1 | SAR11 16S rRNA Phylogenetic tree. Maximum likelihood phylogeny used as the database reference for the taxonomic placement of the retrieved SAR11 ASVs. Subclades are labeled following Giovannoni (2017) and Haro-Moreno et al. (2020) classification.

Supplementary Figure 2 | Hierarchical clustering of the samples based on the phytoplankton ASV profiles. ASVs dendrogram (top) defined by hierarchical clustering of the phytoplankton fraction in the euphotic zone (5–100 m). Heatmap (bottom) represents the relative contribution of each major taxonomic group to the phytoplankton fraction. Based on the dendogram and the samples origin subgroups were defined as indicated by the dashed lines in the heatmap. From left to right: subtropical autumn, SA (subtropical autumn) DCM (Deep-chlorophyll maximum), subpolar autumn, subpolar winter, subpolar late spring, subtropical late spring, subtropical winter, and subtropical early spring.

Supplementary Figure 3 | Phytoplankton multidimensional scaling (MDS) ordination based on Bray-Curtis dissimilarities. Top panel represents the original MDS without the seasonal subdivision presented in Figure 2A (4-panel split). Datasets are colored based on the MDT subregion. Bottom panel represents the original MDS color-coded by the determined biological division of the subregions (Subpolar and Subtropical). In both panels, 50% ellipses are depicted around the centroids of the sample categories. Below we presented the stress analysis of the ordination and the Permutational Multivariate Analysis of Variance that support the described differences between subregions and seasons for the phytoplankton.

Supplementary Figure 4 | Bacterioplankton multidimensional scaling (MDS) ordination based on Bray-Curtis dissimilarities. Top panel represents the original MDS without the seasonal subdivision presented in Figure 2B (4-panel split). Datasets are colored based on the MDT subregion. Bottom panel represents the original MDS color-coded by the determined biological division of the subregions (Subpolar and Subtropical). In both panels, 50% ellipses are depicted around the centroids of the sample categories. Below we presented the stress analysis of the ordination and the Permutational Multivariate Analysis of Variance that support the described differences between subregions and seasons for the phytoplankton.

Supplementary Figure 5 | Covariation network of the 128 phytoplankton and 292 bacterioplankton most abundant ASVs and modularity analysis color coded by Order. Visual representation of the non-directed ASVs covariation network. Nodes are color-coded by Order or the lowest taxonomical hierarchy available in case order was not determined. Congruently to Figure 7, the visual representation of the non-directed ASVs covariation network with the color-coded nodes by module is presented in the bottom panel. Size of the nodes in both panels depicts the log2 of the represented ASV average.

Supplementary Figure 6 | Non-directed covariation networks of each of the modules defined by the modularity analysis of the global network. Nodes are color coded by phylum and labeled using the name of the ASVs these represent and the higher taxonomy resolution (full taxonomy classification available in Supplementary Table 1).

Supplementary Table 1 | Taxonomy table of the ASVs used in the covariation network.

the western North Atlantic. Front. Mar. Sci. 7:227. doi: 10.3389/fmars.2020.

Behrenfeld, M. J., and Boss, E. S. (2018). Student's tutorial on bloom hypotheses in the context of phytoplankton annual cycles. *Glob. Chang. Biol.* 24, 55–77. doi: 10.1111/gcb.13858

Behrenfeld, M. J., Moore, R. H., Hostetler, C. A., Graff, J., Gaube, P., Russell, L. M., et al. (2019). The North Atlantic Aerosol and marine ecosystem study

- (NAAMES): science motive and mission overview. Front. Mar. Sci. 6:122. doi: 10.3389/fmars.2019.00122
- Bolaños, L. M., Karp-Boss, L., Choi, C. J., Worden, A. Z., Graff, J. R., Haëntjens, N., et al. (2020). Small phytoplankton dominate western North Atlantic biomass. ISME J. 14, 1663–1674. doi: 10.1038/s41396-02 0-0636-0
- Brown, M. V., Lauro, F. M., DeMaere, M. Z., Muir, L., Wilkins, D., Thomas, T., et al. (2012). Global biogeography of SAR11 marine bacteria. *Mol. Syst. Biol.* 8:595. doi: 10.1038/msb.2012.28
- Buchan, A., LeCleir, G. R., Gulvik, C. A., and González, J. M. (2014).
 Master recyclers: features and functions of bacteria associated with phytoplankton blooms. *Nat. Rev. Microbiol.* 12, 686–698. doi: 10.1038/nrmicro
- Bunse, C., and Pinhassi, J. (2017). Marine bacterioplankton seasonal succession dynamics. Trends Microbiol. 25, 494–505. doi: 10.1016/j.tim.2016.12.013
- Butts, C. T. (2019). sna: Tools for Social Network Analysis. Avaliable online at: https://cran.r-project.org/package=sna (accessed June 20, 2019).
- Callahan, B. J., McMurdie, P. J., Rosen, M. J., Han, A. W., Johnson, A. J. A., and Holmes, S. P. (2016). DADA2: High-resolution sample inference from Illumina amplicon data. *Nat. Methods* 13:581. doi: 10.1038/nmeth.3869
- Camarena-Gómez, M., Lipsewers, T., Piiparinen, J., Eronen-Rasimus, E., Perez-Quemaliños, D., Hoikkala, L., et al. (2018). Shifts in phytoplankton community structure modify bacterial production, abundance and community composition. Aquat. Microb. Ecol. 81, 149–170. doi: 10.3354/ame 01868
- Carlson, C. A., Giovannoni, S. J., Hansell, D. A., Goldberg, S. J., Parsons, R., Otero, M. P., et al. (2002). Effect of nutrient amendments on bacterioplankton production, community structure, and DOC utilization in the northwestern Sargasso Sea. Aquat. Microb. Ecol. 30, 19–36. doi: 10.3354/Ame 030019
- Carlson, C. A., and Hansell, D. A. (2015). "DOM sources, sinks, reactivity, and budgets," in *Biogeochemistry of Marine Dissolved Organic Matter*, eds D. A. Hansell and C. A. Carlson (San Diego, CA: Academic Press), 65–126. doi: 10.1016/b978-0-12-405940-5.00003-0
- Carlson, C. A., Hansell, D. A., Nelson, N. B., Siegel, D. A., Smethie, W. M., Khatiwala, S., et al. (2010). Dissolved organic carbon export and subsequent remineralization in the mesopelagic and bathypelagic realms of the North Atlantic basin. *Deep Sea Res. Part II Top. Stud. Oceanogr.* 57, 1433–1445. doi: 10.1016/j.dsr2.2010.02.013
- Carlson, C. A., Morris, R., Parsons, R., Treusch, A. H., Giovannoni, S. J., and Vergin, K. (2009). Seasonal dynamics of SAR11 populations in the euphotic and mesopelagic zones of the northwestern Sargasso Sea. *ISME J.* 3, 283–295. doi: 10.1038/ismej.2008.117
- Choi, C. J., Bachy, C., Jaeger, G. S., Poirier, C., Sudek, L., Sarma, V., et al. (2017). Newly discovered deep-branching marine plastid lineages are numerically rare but globally distributed. *Curr. Biol.* 27, R15–R16. doi: 10.1016/j.cub.2016.11. 032
- Choi, C. J., Jimenez, V., Needham, D. M., Poirier, C., Bachy, C., Alexander, M., et al. (2020). Seasonal and geographical transitions in phytoplankton community structure in the Atlantic and Pacific Oceans. Front. Microbiol. 11:542372. doi: 10.3389/fmicb.2020.542372
- Cram, J. A., Chow, C.-E. T., Sachdeva, R., Needham, J. A., Parada, A. E., Steele, J. A., et al. (2015). Seasonal and interannual variability of the marine bacterioplankton community throughout the water column over ten years. *ISME J.* 9, 563–580. doi: 10.1038/ismej.20 14.153
- Csárdi, G., and Nepusz, T. (2006). The igraph software package for complex network research. *InterJ. Complex Syst.* 1695, 1–9.
- Daims, H., Brühl, A., Amann, R., Schleifer, K.-H., and Wagner, M. (1999).
 The domain-specific probe EUB338 is insufficient for the detection of all bacteria: development and evaluation of a more comprehensive probe set. Syst. Appl. Microbiol. 22, 434–444. doi: 10.1016/S0723-2020(99) 80053-8
- Davis, N. M., Proctor, D. M., Holmes, S. P., Relman, D. A., and Callahan, B. J. (2018). Simple statistical identification and removal of contaminant sequences in marker-gene and metagenomics data. *Microbiome* 6:226. doi: 10.1186/ s40168-018-0605-2

- Della Penna, A., and Gaube, P. (2019). Overview of (sub)mesoscale ocean dynamics for the NAAMES field program. *Front. Mar. Sci.* 6:384. doi: 10.3389/fmars.2019. 00384
- Della Penna, A., and Gaube, P. (2020). Mesoscale Eddies structure mesopelagic communities. Front. Mar. Sci. 7:454. doi: 10.3389/fmars.2020.00454
- Delmont, T. O., Kiefl, E., Kilinc, O., Esen, O. C., Uysal, I., Rappe, M. S., et al. (2019). Single-amino acid variants reveal evolutionary processes that shape the biogeography of a global SAR11 subclade. *Elife* 8:e46497. doi: 10.7554/eLife. 46497
- DeLong, E. F., Preston, C. M., Mincer, T., Rich, V., Hallam, S. J., Frigaard, N.-U., et al. (2006). Community genomics among stratified microbial assemblages in the ocean's interior. *Science* 311, 496–503. doi: 10.1126/science.11 20250
- Duarte, C. M. (2015). Seafaring in the 21st century: the Malaspina 2010 circumnavigation expedition. *Limnol. Oceanogr. Bull.* 24, 11–14. doi: 10.1002/ lob.10008
- Ducklow, H. W., Steinberg, D. K., and Buesseler, K. O. (2001). Upper ocean carbon export and the biological pump. *Oceanography* 14, 50–58. doi: 10.5670/oceanog. 2001.06
- Eren, A. M., Maignien, L., Sul, W. J., Murphy, L. G., Grim, S. L., Morrison, H. G., et al. (2013). Oligotyping: differentiating between closely related microbial taxa using 16S rRNA gene data. *Methods Ecol. Evol.* 4, 1111–1119. doi: 10.1111/2041-210X.12114
- Field, K. G., Gordon, D., Wright, T., Rappé, M., Urback, E., Vergin, K., et al. (1997).
 Diversity and depth-specific distribution of SAR11 cluster rRNA genes from marine planktonic bacteria. Appl. Environ. Microbiol. 63, 63–70.
- Flombaum, P., Gallegos, J. L., Gordillo, R. A., Rincón, J., Zabala, L. L., Jiao, N., et al. (2013). Present and future global distributions of the marine Cyanobacteria, Prochlorococcus, and Synechococcus. Proc. Natl. Acad. Sci. U.S.A. 110, 9824– 9829. doi: 10.1073/pnas.1307701110
- Giovannoni, S. J. (2017). SAR11 bacteria: the most abundant plankton in the oceans. Ann. Rev. Mar. Sci. 9, 231–255. doi: 10.1146/annurev-marine-010814-015934
- Giovannoni, S. J., Rappé, M. S., Vergin, K. L., and Adair, N. L. (1996). 16S rRNA genes reveal stratified open ocean bacterioplankton populations related to the green non-sulfur bacteria. *Proc. Natl. Acad. Sci. U.S.A.* 93, 7979–7984. doi: 10.1073/pnas.93.15.7979
- Giovannoni, S. J., and Vergin, K. L. (2012). Seasonality in ocean microbial communities. Science 335, 671–676. doi: 10.1126/science.1198078
- Graff, J. R., and Behrenfeld, M. J. (2018). Photoacclimation responses in subarctic Atlantic phytoplankton following a natural mixing-restratification event. Front. Mar. Sci. 5:209. doi: 10.3389/fmars.2018.00209
- Hansell, D. A., Carlson, C. A., Repeta, D. J., and Schlitzer, R. (2009). Dissolved organic matter in the ocean: a controversy stimulates new insights. *Oceanography* 22, 202–211. doi: 10.5670/oceanog.2009.109
- Haro-Moreno, J. M., Rodriguez-Valera, F., Rosselli, R., Martinez-Hernandez, F., Roda-Garcia, J. J., Gomez, M. L., et al. (2020). Ecogenomics of the SAR11 clade. *Environ. Microbiol.* 22, 1748–1763. doi: 10.1111/1462-2920.14896
- Karsenti, E., Acinas, S. G., Bork, P., Bowler, C., Vargas, C. D., Raes, J., et al. (2011).
 A holistic approach to marine eco-systems biology. *PLoS Biol.* 9:e1001177.
 doi: 10.1371/journal.pbio.1001177
- Kirkham, A. R., Jardillier, L. E., Tiganescu, A., Pearman, J., Zubkov, M. V., and Scanlan, D. J. (2011). Basin-scale distribution patterns of photosynthetic picoeukaryotes along an Atlantic meridional transect. *Environ. Microbiol.* 13, 975–990. doi: 10.1111/j.1462-2920.2010. 02403.x
- Kramer, S. J., Siegel, D. A., and Graff, J. R. (2020). Phytoplankton community composition determined from co-variability among phytoplankton pigments from the NAAMES field campaign. Front. Mar. Sci. 7:215. doi: 10.3389/fmars. 2020.00215
- Kurtz, Z. D., Müller, C. L., Miraldi, E. R., Littman, D. R., Blaser, M. J., and Bonneau, R. A. (2015). Sparse and compositionally robust inference of microbial ecological networks. *PLoS Comput. Biol.* 11:e1004226. doi: 10.1371/ journal.pcbi.1004226
- Landa, M., Blain, S., Christaki, U., Monchy, S., and Obernosterer, I. (2016). Shifts in bacterial community composition associated with increased carbon cycling in a mosaic of phytoplankton blooms. *ISME J.* 10, 39–50. doi: 10.1038/ismej. 2015.105

- Landry, Z., Swan, B. K., Herndl, G. J., Stepanauskas, R., and Giovannoni, S. J. (2017). SAR202 genomes from the dark ocean predict pathways for the oxidation of recalcitrant dissolved organic matter. mBio 8:e00413–17. doi: 10. 1128/mBio.00413-17
- Lane, D. J. (1991). "16S/23S rRNA sequencing," in Nucleic Acid Techniques in Bacterial Systematics, eds E. Stackebrandt and M. Goodfellow (New York, NY: John Wiley & Sons), 115–175.
- Lima-Mendez, G., Faust, K., Henry, N., Decelle, J., Colin, S., Carcillo, F., et al. (2015). Determinants of community structure in the global plankton interactome. *Science* 348, 1262073. doi: 10.1126/science.12 62073
- Liu, R., Wang, L., Liu, Q., Wang, Z., Li, Z., Fang, J., et al. (2018). Depth-resolved distribution of particle-attached and free-living bacterial communities in the water column of the New Britain Trench. Front. Microbiol. 9:625. doi: 10.3389/ fmicb.2018.00625
- Liu, S., Baetge, N., Comstock, J., Opalk, K., Parsons, R. J., Halewood, E., et al. (2020a). Stable isotope probing identifies bacterioplankton lineages capable of utilizing dissolved organic matter across a range of bioavailability. Front. Microbiol. 11:580397. doi: 10.3389/fmicb.2020. 580397
- Liu, S., Parsons, R., Opalk, K., Baetge, N., Giovannoni, S., Bolaños, L. M., et al. (2020b). Different carboxyl-rich alicyclic molecules proxy compounds select distinct bacterioplankton for oxidation of dissolved organic matter in the mesopelagic Sargasso Sea. *Limnol. Oceanogr.* 65, 1532–1553. doi: 10.1002/lno. 11405
- Love, M. I., Huber, W., and Anders, S. (2014). Moderated estimation of fold change and dispersion for RNA-seq data with DESeq2. Genome Biol. 15:550. doi: 10.1186/s13059-014-0550-8
- Luria, C. M., Amaral-Zettler, L. A., Ducklow, H. W., Repeta, D. J., Rhyne, A. L., and Rich, J. J. (2017). Seasonal shifts in bacterial community responses to phytoplankton-derived dissolved organic matter in the Western Antarctic Peninsula. Front. Microbiol. 8:2117. doi: 10.3389/fmicb.2017. 02117
- Martin, M. (2011). Cutadapt removes adapter sequences from highthroughput sequencing reads. EMBnet J. 17:10. doi: 10.14806/ej.17. 1.200
- Martin, P., Lampitt, R. S., Jane Perry, M., Sanders, R., Lee, C., and D'Asaro, E. (2011). Export and mesopelagic particle flux during a North Atlantic spring diatom bloom. *Deep Sea Res.* 58, 338–349. doi: 10.1016/j.dsr.2011.
- Massana, R., Pedrós, A. C., Casamayor, E. O., and Gasol, J. M. (2001). Changes in marine bacterioplankton phylogenetic composition during incubations designed to measure biogeochemically significant parameters. *Limnol. Oceanogr.* 46, 1181–1188. doi: 10.4319/lo.2001.46. 5.1181
- McMurdie, P. J., and Holmes, S. (2013). Phyloseq: an R Package for reproducible interactive analysis and graphics of microbiome census data. *PLoS One* 8:e61217. doi: 10.1371/journal.pone.0061217
- Meon, B., and Kirchman, D. L. (2001). Dynamics and molecular composition of dissolved organic material during experimental phytoplankton blooms. Mar. Chem. 75, 185–199. doi: 10.1016/S0304-4203(01) 00036-6
- Milici, M., Tomasch, J., Wos-Oxley, M. L., Wang, H., Jáuregui, R., Camarinha-Silva, A., et al. (2016). Low diversity of planktonic bacteria in the tropical ocean. Sci. Rep. 6:19054. doi: 10.1038/srep19054
- Moeseneder, M. M., Winter, C., and Herndl, G. J. (2001). Horizontal and vertical complexity of attached and free-living bacteria of the eastern Mediterranean Sea, determined by 16S rDNA and 16S rRNA fingerprints. *Limnol. Oceanogr.* 46, 95–107. doi: 10.4319/lo.2001.46. 1.0095
- Morán, X. A. G., López-Urrutia, Á, Calvo-Díaz, A., and Li, W. K. W. (2010). Increasing importance of small phytoplankton in a Warmer Ocean. *Glob. Change Biol.* 16, 1137–1144. doi: 10.1111/j.1365-2486.2009. 01960.x
- Morison, F., Harvey, E., Franzè, G., and Menden-Deuer, S. (2019). Storm-induced predator-prey decoupling promotes springtime accumulation of North Atlantic phytoplankton. Front. Mar. Sci. 6:608. doi: 10.3389/fmars.2019. 00608

- Needham, D. M., and Fuhrman, J. A. (2016). Pronounced daily succession of phytoplankton, archaea and bacteria following a spring bloom. *Nat. Microbiol.* 1: 16005. doi: 10.1038/nmicrobiol.2016.5
- Nelson, C. E., Carlson, C. A., Ewart, C. S., and Halewood, E. R. (2013).
 Community differentiation and population enrichment of Sargasso Sea bacterioplankton in the euphotic zone of a mesoscale modewater eddy. *Environ. Microbiol.* 16, 871–887. doi: 10.1111/1462-2920.
 12241
- Nelson, C. E., Goldberg, S. J., Kelly, L. W., Haas, A. F., Smith, J. E., Rohwer, F., et al. (2014). Coral and macroalgal exudates vary in neutral sugar composition and differentially enrich reef bacterioplankton lineages. *ISME J.* 7, 962–979. doi: 10.1038/ismej.2012.161
- Quast, C., Pruesse, E., Yilmaz, P., Gerken, J., Schweer, T., Yarza, P., et al. (2012). The SILVA ribosomal RNA gene database project: improved data processing and web-based tools. *Nucleic Acids Res.* 41, 590–596. doi: 10.1093/nar/ gks1219
- Rappé, M. S., Suzuki, M. T., Vergin, K. L., and Giovannoni, S. J. (1998). Phylogenetic diversity of ultraplankton plastid small-subunit rRNA genes recovered in environmental nucleic acid samples from the Pacific and Atlantic coasts of the United States. Appl. Environ. Microbiol. 64, 294–303. doi: 10.1128/ AEM.64.1.294-303.1998
- Romera-Castillo, C., Letscher, R. T., and Hansell, D. A. (2016). New nutrients exert fundamental control on dissolved organic carbon accumulation in the surface Atlantic Ocean. *Proc. Natl. Acad. Sci. U.S.A.* 113, 10497–10502. doi: 10.1073/pnas.1605344113
- Sanders, R., Henson, S. A., Koski, M., De La Rocha, C. L., Painter, S. C., Poulton, A. J., et al. (2014). The biological carbon pump in the North Atlantic. *Prog. Oceanogr.* 129, 200–218. doi: 10.1016/j.pocean.2014. 05.005
- Saw, J. H. W., Nunoura, T., Hirai, M., Takaki, Y., Parsons, R., Michelsen, M., et al. (2020). Pangenomics analysis reveals diversification of enzyme families and niche specialization in globally abundant SAR202 bacteria. mBio 11:e02975-19. doi: 10.1128/mBio.02975-19
- Sieracki, M. E., Verity, P. G., and Stoecker, D. K. (1993). Plankton community response to sequential silicate and nitrate depletion during the 1989 North Atlantic spring bloom. *Deep Sea Res.* 40, 213–225. doi: 10.1016/0967-0645(93) 90014-F
- Signori, C. N., Pellizari, V. H., Enrich-Prast, A., and Sievert, S. M. (2018). Spatiotemporal dynamics of marine bacterial and archaeal communities in surface waters off the northern Antarctic Peninsula. *Deep Sea Res.* 149, 150–160. doi: 10.1016/j.dsr2.2017.12.017
- Sudek, S., Everroad, R. C., Gehman, A. L., Smith, J. M., Poirier, C. L., Chavez, F. P., et al. (2015). Cyanobacterial distributions along a physico-chemical gradient in the Northeastern Pacific Ocean. *Environ. Microbiol.* 17, 3692–3707. doi: 10.1111/1462-2920.12742
- Sunagawa, S., Acinas, S. G., Bork, P., Bowler, C., Eveillard, D., Gorsky, G., et al. (2020). Tara Oceans: towards global ocean ecosystems biology. *Nat. Rev. Microbiol.* 18, 428–445. doi: 10.1038/s41579-020-0364-5
- Swan, B. K., Martinez-Garcia, M., Preston, C. M., Sczyrba, A., Woyke, T., Lamy, D., et al. (2011). Potential for chemolithoautotrophy among ubiquitous bacteria lineages in the dark ocean. *Science* 333, 1296–1300. doi: 10.1126/science. 1203690
- Teeling, H., Fuchs, B. M., Becher, D., Klockow, C., Gardebrecht, A., Bennke, C. M., et al. (2012). Substrate-controlled succession of marine bacterioplankton populations induced by a phytoplankton bloom. *Science* 336, 608–611. doi: 10.1126/science.1218344
- Thompson, J. D., Higgins, D. G., and Gibson, T. J. (1994). CLUSTAL W: improving the sensitivity of progressive multiple sequence alignment through sequence weighting, position-specific gap penalties and weight matrix choice. *Nucleic Acids Res.* 22, 4673–4680. doi: 10.1093/nar/22. 22.4673
- Thornton, D. C. O. (2014). Dissolved organic matter (DOM) release by phytoplankton in the contemporary and future ocean. Eur. J. Phycol. 49, 20–46. doi: 10.1080/09670262.2013.875596
- Treusch, A. H., Vergin, K. L., Finlay, L. A., Donatz, M. G., Burton, R. M., Carlson, C. A., et al. (2009). Seasonality and vertical structure of microbial communities in an ocean gyre. *ISME J.* 3, 1148–1163. doi: 10.1038/ismej.

- Vergin, K. L., Beszteri, B., Monier, A., Thrash, J. C., Temperton, B., Treusch, A. H., et al. (2013). High-resolution SAR11 ecotype dynamics at the Bermuda Atlantic Time-series Study site by phylogenetic placement of pyrosequences. *ISME J.* 7, 1322–1332. doi: 10.1038/ismej.2013.32
- Wear, E. K., Carlson, C. A., James, A. K., Brzezinski, M. A., Windecker, L. A., and Nelson, C. E. (2015a). Synchronous shifts in dissolved organic carbon bioavailability and bacterial community responses over the course of an upwelling-driven phytoplankton bloom: bloom-induced shifts in DOC availability. Limnol. Oceanogr. 60, 657–677. doi: 10.1002/lno.10042
- Wear, E. K., Carlson, C. A., Windecker, L. A., and Brzezinski, M. A. (2015b). Roles of diatom nutrient stress and species identity in determining the short- and long-term bioavailability of diatom exudates to bacterioplankton. *Mar. Chem.* 177, 335–348. doi: 10.1016/j.marchem.2015. 09.001
- Wickham, H. (2016). ggplot2: Elegant Graphics for Data Analysis. Berlin: Springer. Yang, B., Boss, E. S., Haëntjens, N., Long, M. C., Behrenfeld, M. J., Eveleth, R., et al. (2020). Phytoplankton phenology in the north atlantic: insights from

- profiling float measurements. Front. Mar. Sci. 7:139. doi: 10.3389/fmars.2020. 00139
- Yilmaz, P., Yarza, P., Rapp, J. Z., and Glöckner, F. O. (2016). Expanding the world of marine bacterial and archaeal clades. Front. Microbiol. 6:1524. doi: 10.3389/ fmicb 2015.01524

Conflict of Interest: The authors declare that the research was conducted in the absence of any commercial or financial relationships that could be construed as a potential conflict of interest.

Copyright © 2021 Bolaños, Choi, Worden, Baetge, Carlson and Giovannoni. This is an open-access article distributed under the terms of the Creative Commons Attribution License (CC BY). The use, distribution or reproduction in other forums is permitted, provided the original author(s) and the copyright owner(s) are credited and that the original publication in this journal is cited, in accordance with accepted academic practice. No use, distribution or reproduction is permitted which does not comply with these terms.